Regular Article

IMMUNOBIOLOGY

Cell-intrinsic regulation of murine dendritic cell function and survival by prereceptor amplification of glucocorticoid

Annelise Soulier,[1] Sandra M. Blois,[2] Shivajanani Sivakumaran,[2] Farnaz Fallah-Arani,[2] Stephen Henderson,[3] Barry Flutter,[2] Elizabeth H. Rabbitt,[4] Paul M. Stewart,[4] Gareth G. Lavery,[4] Clare Bennett,[2] S. John Curnow,[1] and Ronjon Chakraverty[2]

[1]School of Immunity and Infection, Centre for Translational Inflammation Research, College of Medical and Dental Sciences, University of Birmingham, Birmingham, United Kingdom; [2]Transplantation Immunology Group, Department of Haematology, Cancer Institute and Institute of Immunity and Transplantation, University College London, London, United Kingdom; [3]Cancer Research UK Viral Oncology Group, University College London, London, United Kingdom; and [4]School of Clinical and Experimental Medicine, College of Medical and Dental Sciences, University of Birmingham, Birmingham, United Kingdom

Key Points

- Murine dendritic cell populations are highly proficient in amplifying local glucocorticoid concentrations.
- This property is critical in regulating dendritic cell survival and functions in vivo.

Although the inhibitory effects of therapeutic glucocorticoids (GCs) on dendritic cells (DCs) are well established, the roles of endogenous GCs in DC homeostasis are less clear. A critical element regulating endogenous GC concentrations involves local conversion of inactive substrates to active 11-hydroxyglucocorticoids, a reduction reaction catalyzed within the endoplasmic reticulum by an enzyme complex containing 11β-hydroxysteroid dehydrogenase type 1 (11βHSD1) and hexose-6-phosphate dehydrogenase (H6PDH). In this study, we found that this GC amplification pathway operates both constitutively and maximally in steady state murine DC populations and is unaffected by additional inflammatory stimuli. Under physiologic conditions, 11βHSD1-H6PDH increases the sensitivity of plasmacytoid DCs (pDCs) to GC-induced apoptosis and restricts the survival of this population through a cell-intrinsic mechanism. Upon CpG activation, the effects of enzyme activity are overridden, with pDCs becoming resistant to GCs and fully competent to release type I interferon. CD8α⁺ DCs are also highly proficient in amplifying GC levels, leading to impaired maturation following toll-like receptor–mediated signaling. Indeed, pharmacologic inhibition of 11βHSD1 synergized with CpG to enhance specific T-cell responses following vaccination targeted to CD8α⁺ DCs. In conclusion, amplification of endogenous GCs is a critical cell-autonomous mechanism for regulating the survival and functions of DCs in vivo. (Blood. 2013;122(19):3288-3297)

Introduction

Glucocorticoids (GCs) are lipid hormones that signal through an intracellular GC receptor (GR) and play a major role in immune system homeostasis.[1] Potential targets of GCs are dendritic cells (DCs),[2] heterogeneous populations of specialized antigen-presenting cells. For example, in vitro treatment of myeloid DCs with GCs impairs their capacity to process antigens or to express proinflammatory cytokines.[3-7] Plasmacytoid DCs (pDCs) are also exquisitely sensitive to GCs and rapidly undergo apoptosis following exposure.[8] These findings largely derive from studies using exogenous and/or synthetic GCs, often at supraphysiologic concentrations. In contrast, relatively little is known about how endogenous GCs regulate DC functions and survival in vivo.

Although the hypothalamic-pituitary-adrenal axis performs the major role in controlling systemic GC concentrations, how this affects levels within tissues is not known.[9] Microenvironment cellular responses are fine tuned at both receptor[10] and prereceptor levels.[11] Variant GR isoforms arising through alternate splicing or translation initiation confer distinct transcriptional responses in individual cell populations.[10,12] Prereceptor regulation of local GC bioavailability may be achieved either by de novo synthesis of GCs from

cholesterol (eg, in the gut[13] or thymus[14]), or by a second mechanism with broader participation that involves the conversion of 11-oxoglucocorticoids that bind the GR with very low affinity (eg, cortisone, 11-dehydrocorticosterone) to 11-hydroxyglucocorticoids that bind GR with high affinity (eg, cortisol, corticosterone).[11] This reduction reaction is catalyzed by 11β-hydroxysteroid dehydrogenase type 1 (11βHSD1), an enzyme located within the endoplasmic reticulum of cells of several tissues, including the liver, adipose tissue, lungs, and the immune system.[11] Transgenic studies involving selective overexpression of 11βHSD1 in the liver and adipose tissue have demonstrated tissue-specific effects of increased local GC bioavailability.[15] 11βHSD1 has cooperative and physical interactions with a second enzyme, hexose-6-phosphate dehydrogenase (H6PDH), which provides a ready supply of reduced nicotinamide adenine dinucleotide phosphate for the reductase activity.[16-18]

We have previously shown that the 11βHSD1-H6PDH pathway is expressed in human monocyte-derived DCs.[19] Increases in the bioavailability of cortisol act via autocrine and/or paracrine mechanisms to block DC functions.[19] To test whether these findings are relevant in vivo, we have now evaluated murine DC populations in

contexts in which the 11βHSD1-H6PDH pathway is either intact or disabled. We show for the first time that both pDCs and CD8α⁺ DCs are highly proficient in generating active forms of GCs and that this property has critical cell-autonomous roles in regulating DC survival and function.

Materials and methods

Animals

Experiments were performed according to Home Office Guidance (Animals [Scientific Procedures Act] 1986) and approved by the local ethics committee. $H6pdh^{-/-}$ mice have been previously reported.[20]

Bone marrow transplantation

12-week-old female B6 $H6pdh^{+/+}$ mice received 11 Gy x-ray irradiation before intravenous injection of $H6pdh^{+/+}$ (CD45.1) and $H6pdh^{-/-}$ (CD45.2) bone marrow (BM) alone or as a 1:1 mix (total dose, 5×10^6). Chimeric mice were used for experiments at ~3 months following reconstitution.

Isolation of DCs

Splenic DCs were isolated by immunomagnetic separation that used CD11c MicroBeads or plasmacytoid, CD8⁺ or CD4⁺ DC Isolation kits (Miltenyi Biotec, Woking, UK) or by flow sorting on a FACSAria (BD Biosciences, Oxford, UK). Granulocyte macrophage colony-stimulating factor (GM-CSF)–propagated BM DCs and Fms-like tyrosine kinase 3 ligand–generated BM-derived pDCs were cultured as described previously.[21]

Media and other reagents

Medium was RPMI 1640 (Invitrogen, Paisley, UK), supplemented with 10% heat-inactivated and steroid-free fetal calf serum (Valeant Pharmaceuticals, Quebec, Canada). Steroid hormones were removed by using dextran-coated charcoal (Sigma-Aldrich, Dorset, UK). 11-dehydrocorticosterone and corticosterone were from Steraloids Inc. (Newport, RI). OVA$_{257-264}$ and OVA$_{323-339}$ peptides were from ProImmune (Oxford, UK) and AnaSpec (Fremont, CA), respectively. Toll-like receptor (TLR) agonists were from Invivogen (Toulouse, France) and were used at the concentrations indicated in the Figure legends.

Corticosterone assays

Purified DC subsets (2×10^5 cells per well in 200 μL) were incubated in the presence or absence of 11-dehydrocorticosterone at 10^{-6} M or 10^{-7} M in 96-well culture plates. After 18 hours, plates were centrifuged and supernatant was assayed by using Corticosterone Enzyme Immunoassay Kit (Cayman Chemical Company, Ann Arbor, MI) according to the manufacturer's procedures to assess the concentrations of corticosterone (limit of detection: 80% B/B$_0$:30 pg/mL; sensitivity: 50% B/B$_0$:150 pg/mL, where B = signal − intercept constant and B$_0$ = maximal signal − intercept constant). Enzyme activity assays were performed by thin layer chromatography of supernatants following incubation of cells with radiolabeled GCs, as described previously.[19]

Quantitative reverse-transcription polymerase chain reaction

Messenger RNA was extracted by using the RNeasy Micro Kit, and complementary DNA was synthesized by using the QuantiTect Reverse Transcription Kit (both Qiagen, Manchester, UK). $11bhsd1$ and $H6pd$ complementary DNAs were amplified by using commercially available QuantiTect Primer Assay kits (Qiagen) in a SYBR Green-based reverse-transcription polymerase chain reaction (Qiagen) on an ABI7400 cycler (Applied Biosystems, Paisley, UK). Transcripts of test genes ("gene X") were quantified relative to the abundance of housekeeping genes by the change in threshold (C$_T$) method (relative expression, $2^{-(CT(gene\ X) - CT(housekeeping))}$).

IFN-α enzyme-linked immunosorbent assay

BM pDC subsets (2×10^5 cells per well) were cultured overnight ± CpG 2216 at 2 μM and ± 11-dehydrocorticosterone or corticosterone at 10^{-7} M. After 18 hours, plates were centrifuged and supernatant was assayed by using VeriKine Mouse Interferon Alpha (IFN-α) Enzyme-Linked Immunosorbent Assay Kit (PBL Interferon Source, Piscataway NJ) according to the manufacturer's instructions.

Flow cytometry

The following monoclonal antibodies, isotype controls, and flow cytometric reagents were from eBioscience (Hatfield, UK): Annexin V Apoptosis Detection Kit, anti-CD8a (53.6.7), anti-CD11c (N418), anti-CD11b (M1/70), anti-CD45.1 (A20), anti-CD86 (GL1), anti-B220 (RA3-6B2), anti-major histocompatibility complex (MHC) class II (M5/114.15.2), anti-sialic acid binding immunoglobulin-like lectin H (SiglecH; Ebio440c), and IFN-γ (XMG1.2). Anti-plasmacytoid dendritic cell antigen-1 (PDCA-1) (JF05-1C241) was from Miltenyi Biotec. Samples were run on a BD Fortessa (BD Biosciences, Oxford, UK), and analysis was performed by using FlowJo software (TreeStar Inc.). H-2Kb (SIINFEKL) pentamer was from ProImmune, Oxford, UK.

ELISPOT and in vivo cytotoxicity

Enzyme-linked immunospot (ELISPOT) and in vivo cytotoxicity were performed as described previously.[22]

Anti-DEC205:OVA immunization

Anti-DEC205:OVA was a gift from Ralph Steinman (Rockefeller University, New York, NY) and was produced and used for immunization as previously reported.[23] Carbenoxalone was from Sigma-Aldrich, Dorset, UK.

Statistics

Statistical comparisons were made by using a two-tailed Student t test for parametric data and a two-tailed Mann-Whitney U test for nonparametric data.

Results

Expression of GC biosynthetic pathway enzymes in DCs and DC progenitors

By using published transcriptional array data on mononuclear phagocytes, including DCs and macrophages and their progenitors,[24] we initially compared expression of genes encoding enzymes that participate in the amplification arm of the cortisol-cortisone shuttle ($Hsd11b1$ and $H6pd$) with genes encoding enzymes involved in de novo GC biosynthesis from cholesterol ($Cyp11a1$, $Hsd3b1$, $Cyp21a1$, $Cyp11b1$) (Figure 1A, top). As shown in the heat map in Figure 1A (bottom) and scatter plots in Figure 1B, the patterns of expression for genes within the de novo synthesis group were closely correlated with each other, indicative of coordinate regulation. Gene expression patterns for the shuttle enzymes ($Hsd11b1$ and $H6pd$) correlated poorly with those of the de novo synthesis group, indicating that they are regulated separately (Figure 1B). The value of R^2 was also significantly lower in the comparisons of $Hsd11b1$ versus $H6pd$ gene expression (Figure 1B). In part, this related to very high levels of $Hsd11b1$ messenger RNA in pDCs in comparison with all other groups (Figure 1C-D).

To test the enzyme activity of the 11βHSD1-H6PDH complex, we first sorted pooled CD11c^{high} DCs from the spleens of 10-week-old B6 female mice and evaluated their capacity to reduce inactive 11-dehydrocorticosterone (denoted as "A") to corticosterone, the active form of GC in rodents (conventionally denoted as "B"). As shown in Figure 2A, CD11c^{high} DCs demonstrated significant reductase activity ex vivo, albeit at lower levels than CD4⁺ T cells, which were used as a positive control.[25] By using a competitive
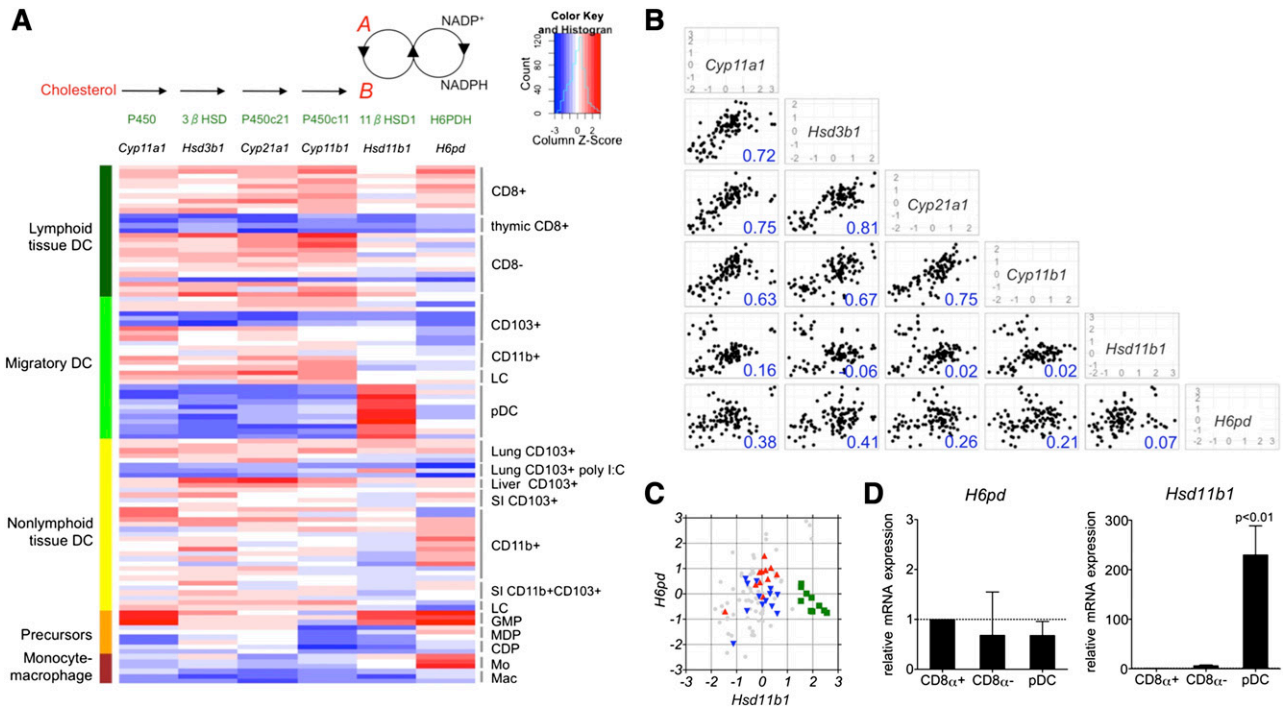
Figure 1. Gene expression of steroid biosynthetic enzymes in murine DCs and their progenitors. (A, top) Steroid biosynthetic pathway is shown for generation of corticosterone ("*B*") from cholesterol or from 11-dehydrocorticosterone ("*A*"). Individual steps in biosynthesis are catalyzed by enzymes shown: P450, cholesterol side chain–cleaving enzyme; 3βHSD, 3β-hydroxysteroid dehydrogenase; P450c21, 21-hydroxylase; P450c11, 11β-hydroxylase; 11βHSD1; and H6PDH. (A, bottom) Heat map showing expression of corresponding genes (in order from top to bottom) from (1) lymphoid tissue DCs: CD8α^+CD11b$^-$ DCs derived from spleen and lymph nodes, thymic CD8α^+ DCs, and CD8α^-CD11b$^+$ DCs derived from spleen and lymph nodes; (2) migratory DCs: CD103$^+$CD11b$^-$, CD103$^-$CD11b$^+$, Langerhans cells (LCs) from draining lymph nodes, and pDCs from spleen and lymph nodes; (3) nonlymphoid tissue DCs: lung CD103$^+$CD11b$^-$ DCs with or without prior polyinosinic:polycytidylic acid (poly I:C) treatment in vivo; liver and small intestinal (SI) CD103$^+$CD11b$^-$ DCs; lung, liver, SI, and kidney CD103$^-$CD11b$^+$ DCs; SI CD103$^+$CD11b$^+$ DCs; and LCs within epidermis; (4) myeloid progenitors: GMP, granulocyte-macrophage progenitor; MDP, macrophage-dendritic cell progenitor; and CDP, common dendritic cell progenitor; and (5) monocytes (Mo) and macrophages (Mac). Methods and selection markers used to isolate individual subsets are available from the Immunological Gene Project.[24] (B) Scatter plots showing gene expression (mean centered log$_2$ expression units) in relation to the mean of the whole data set for individual steroid biosynthetic genes. Values in bottom right corner of each plot show the coefficient of determination (R^2) for each x-y comparison. (C) Graph showing mean centered relative expression of *H6pd* and *Hsd11b1* in whole data set (light gray), with expressions highlighted in color for pDC (green squares), CD8α^+ DC (red upward triangles) and CD8α^- DC (blue downward triangles) subsets. (D) Graphs showing *H6pd* and *Hsd11b1* messenger RNA (mRNA) expression as evaluated by quantitative reverse-transcription polymerase chain reaction in CD8α^- DCs (n = 3 to 4) and pDCs (n = 3 to 6), relative to CD8α^+ DCs (n = 3 to 4). *P* value represents comparison of pDCs to each of the other subsets.

enzyme immunoassay to detect the accumulation of *B* in culture supernatants, we found that both pDCs and pooled CD11c^{high} DCs were able to generate *B* when *A* was added to the media (Figure 2B). To test whether *A*→*B* conversion was dependent upon the shuttle enzyme complex, we incubated DCs from *H6pdh*$^{-/-}$ mice and *H6pdh*$^{+/+}$ littermate controls with *A* and determined the accumulation of *B*. Lack of H6PDH is predicted to prevent generation of nicotinamide adenine dinucleotide phosphate within the endoplasmic reticulum, thus disabling the reductase activity of 11βHSD1.[20] As shown in Figure 2C, *H6pdh*$^{+/+}$ pDCs and CD11c^{high} DCs converted *A*→*B* efficiently, whereas this activity was reduced in the corresponding subsets from *H6pdh*$^{-/-}$ mice.

11βHSD1-H6PDH complex activities of individual DC subsets in steady and inflammatory states

We consistently observed greater conversion of *A*→*B* by pDCs compared with pooled CD11c^{high} DCs (12 342 ± 5924 pg/10^6 cells vs 4744 ± 1914 pg/10^6 cells; *P* < .001; n = 11 to 16), a finding that correlated with their high expression levels of *Hsd11b1*. Most of the reductase activity within the pooled CD11c^{high} DC group was derived from CD8α^+ DCs, which possessed more than a 10-fold greater reductase activity than CD8α^- DCs, although the latter subset still converted *A*→*B* at levels above baseline (Figure 2D-E and not depicted).

To determine whether inflammatory cues would influence the activity of the 11βHSD1-H6PDH complex of splenic DC subsets in vivo, we treated wild-type B6 mice with various TLR agonists or phosphate-buffered saline (PBS), and at 18 hours, we sorted pDCs (± CpG) and individual CD8α^+ and CD8α^- DC subsets (± polyinosinic:polycytidylic acid, lipopolysaccharide [LPS], Flagellin, and CpG) before evaluating their capacity to convert *A*→*B* in short-term cultures ex vivo. As shown in Figure 2D, the 11βHSD1 reductase activities were essentially unaltered following TLR agonist treatment in each of the subsets. We have also shown that human DCs downregulate 11βHSD1 reductase activity upon cross-linking of the CD40 receptor in vitro.[19] To determine whether a similar loss of reductase activity occurred in vivo, we treated mice with agonistic anti-CD40 antibody before purifying DCs and estimating 11βHSD1 function. As shown in Figure 2E, no significant changes in reductase activity were observed. These data suggest that although 11βHSD1-H6PDH activity may vary according to each DC subset, this level represents a default setting unaffected by activation via several proinflammatory stimuli.

Survival of pDCs is regulated by H6PDH in the steady state but not following activation

Therapeutic and stress-related endogenous GC concentrations regulate pDC functions at the level of survival.[26] Because pDCs were
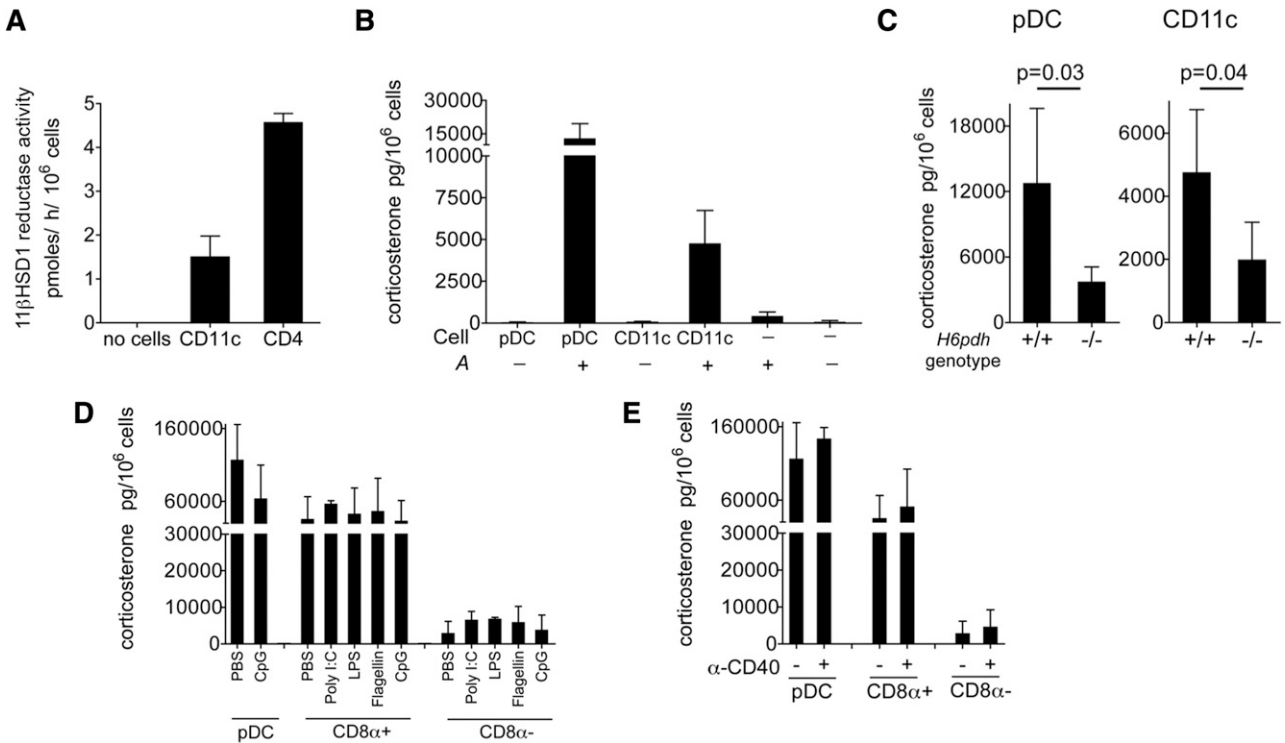
Figure 2. Prereceptor amplification of corticosterone by splenic DC subsets. (A) Estimated 11βHSD1 reductase activity of CD11c$^+$ DCs and CD4 cells (n = 4 per group; 2 independent experiments). (B) Corticosterone generation after 18 hours of pDC or CD11c$^+$ DC culture in the presence or absence of A at 10^{-7} M (n = 10 to 11 per group). (C) Corticosterone in pDCs (n = 4 to 10 per group) or pooled CD11c$^+$ DCs (n = 3 to 11 per group) from spleens of $H6pdh^{-/-}$ mice or $H6pdh^{+/+}$ littermate controls. Data in Figure 2B-C are derived from 3 or more independent experiments. (D) Wild-type B6 mice received phosphate-buffered saline (PBS) or the indicated TLR agonists by intraperitoneal injections (CpG, 150 μg; poly I:C, 100 μg; LPS, 10 μg; Flagellin, 5 μg) 18 hours prior to pDC, CD8$^+$ DC, and CD8α$^-$ DC isolation from the spleen (n = 3 per group per condition; data from 2 independent experiments). Graph shows mean ± standard deviation (SD) corticosterone generation in each experimental group after exposure to A at 10^{-6} M (rather than 10^{-7} M as in Figure 2B-C). Higher concentrations of input A were used to permit detection of B produced by CD8α$^-$ DCs. (E) Wild-type B6 mice received PBS or 50 μg anti-CD40 agonist antibody 18 hours prior to isolation of DC subsets from the spleen (n = 3 per group per condition; data from 2 independent experiments). Graph shows mean ± SD corticosterone generation after exposure to A at 10^{-6} M in each experimental group.

highly proficient at $A{\rightarrow}B$ conversion, we hypothesized that this activity may also influence pDC survival in the steady state. To test this concept, we first generated BM-derived pDCs from $H6pdh^{-/-}$ mice and $H6pdh^{+/+}$ littermate controls and then exposed them to physiologically relevant concentrations of A or B (10^{-7} M) or vehicle alone before evaluating cell viability by Annexin V and propidium iodide (PI) staining after overnight culture. Relative to controls, exposure of $H6pdh^{+/+}$ and $H6pdh^{-/-}$ pDCs to B at 10^{-7} M induced apoptosis to a similar extent (Figure 3A-B). However, whereas exposure of $H6pdh^{+/+}$ pDCs to A reduced overall viability (consistent with efficient $A{\rightarrow}B$ conversion), it had little effect upon $H6pdh^{-/-}$ pDC viability. Because B can diffuse out of cells (as shown in Figure 2B), pDCs could be sensitive to autocrine and/or paracrine effects of $A{\rightarrow}B$ conversion. To test the sensitivity of pDCs to paracrine effects, we mixed $H6pdh^{+/+}$ (CD45.1) and $H6pdh^{-/-}$ (CD45.2) pDCs at a 1:1 ratio before overnight culture in A or B at 10^{-7} M or vehicle alone. As shown in Figure 3B, $H6pdh^{-/-}$ pDCs were now as prone to apoptosis in the presence of A as $H6pdh^{+/+}$ pDCs, indicating sensitivity to paracrine generation of B.

Activation of pDCs through TLR7/9 increases resistance to GC-induced apoptosis.[8,26] To determine the effect of $A{\rightarrow}B$ conversion upon viability in activated pDCs, $H6pdh^{+/+}$ and $H6pdh^{-/-}$ pDCs were exposed to A in the presence of CpG 2216 overnight. As shown in Figure 3A-B, viabilities of $H6pdh^{+/+}$ and $H6pdh^{-/-}$ pDCs were very similar, indicating that H6PDH does not regulate pDC survival following TLR9 activation. Following CpG stimulation, neither surface expression of CD86 and MHC class II, nor the in

vitro capacity to generate IFN-α differed between $H6pdh^{+/+}$ and $H6pdh^{-/-}$ pDCs cultured at physiologic concentrations of A or B (Figure 3C and not depicted).

These data suggested that survival of pDCs in vivo had the potential to be regulated by 11βHSD1-H6PDH complex in the steady state, but that this function would be negated following immune activation with CpG. To test this hypothesis, we initially compared the frequency of pDCs in $H6pdh^{-/-}$ mice and $H6pdh^{+/+}$ littermate controls but found no differences (Figure 4A). However, interpreting these data are problematic because $H6pdh^{-/-}$ mice have greater than twofold elevated systemic levels of B as a consequence of unregulated hypothalamic-pituitary–mediated feedback.[27] To overcome this issue, we generated BM chimeras by reconstituting lethally irradiated $H6pdh^{+/+}$ mice with either $H6pdh^{+/+}$ or $H6pdh^{-/-}$ BM before evaluating pDC numbers 12 weeks after immune reconstitution. As shown in Figure 4B, we again observed no difference in the frequencies or absolute numbers (data not shown) of pDCs in the spleen or lymph node, indicating that H6PDH does not have a cell-intrinsic role in regulating the total pool size at these sites. In order to evaluate whether the activity of the 11βHSD1-H6PDH complex confers a cell-intrinsic effect on pDC survival, we adjusted the experimental design in Figure 4B by reconstituting irradiated B6 female mice with a 50:50 mix of $H6pdh^{+/+}$ and $H6pdh^{-/-}$ BM. As shown in Figure 4C, we observed a consistent competitive advantage for splenic pDCs derived from $H6pdh^{-/-}$ compared with $H6pdh^{+/+}$ BM (mean ratio, 2.5 ± 0.8) to an extent that was greater than that for CD3 cells (mean ratio, 0.9 ± 0.3; P = .004) or neutrophils (mean ratio, 1.3 ± 0.4;
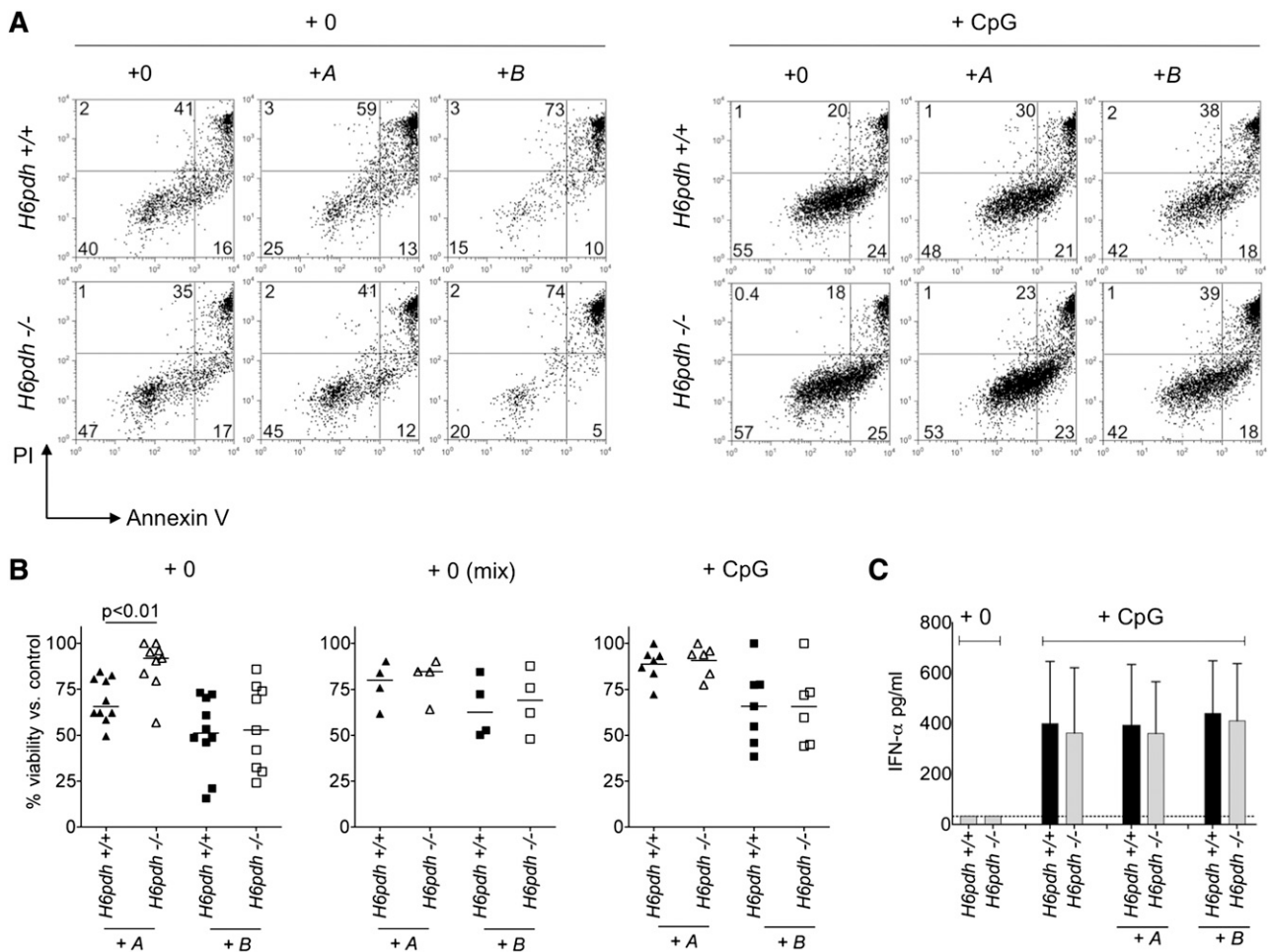
Figure 3. Prereceptor amplification of corticosterone increases apoptosis of pDCs. (A) $H6pdh^{+/+}$ and $H6pdh^{-/-}$ pDCs were cultured overnight in normal media alone (+0) or in the presence of 10^{-7} M 11-dehydrocorticosterone (+A) or 10^{-7} M corticosterone (+B) $\pm$ CpG 2216 at 2 μM before evaluation of cell viability by Annexin V and propidium iodide (PI) staining. (A) Representative flow cytometric plots showing Annexin V and PI staining ($\pm$ CpG 2216). (B) Summary data showing viability of $H6pdh^{+/+}$ and $H6pdh^{-/-}$ pDCs as a percentage of control cultures without addition of A or B or CpG. (Left) pDC viability in the presence of A or B in the absence of CpG. (Middle) Viability of $H6pdh^{-/-}$ (CD45.2) and $H6pdh^{+/+}$ (CD45.1) pDCs when cultured together at a 1:1 ratio in the presence of A or B but in the absence of CpG. (Right) pDC viability in the presence of CpG and either A or B. Data derived from 2 to 3 independent experiments. (C) Mean $\pm$ SD IFN-α levels detected in culture supernatants of $H6pdh^{-/-}$ or $H6pdh^{+/+}$ littermate-derived pDCs following 18 hours of exposure to nil or to CpG 2216 in the presence or absence of 10^{-7} M A or 10^{-7} M B. Data derived from 3 independent experiments (n = 3 per group).

$P = .02$). Steady-state ratios of knockout to wild-type CD11c^{high} cells also trended slightly higher than other myeloid cells (eg, CD11c^{high} cells, mean ratio, 1.7 ± 0.4 vs neutrophils, 1.3 ± 0.4; $P = .06$), but not to the same extent that we had observed for pDCs. To determine whether 11βHSD1 reductase would influence pDC survival under CpG-induced inflammatory conditions, we treated mixed chimeras with CpG 1826 by intraperitoneal injection, and 24 hours later, we evaluated the ratio of $H6pdh^{-/-}$ to $H6pdh^{+/+}$ pDCs from the spleen. In BM chimeras, absolute numbers of pDCs in the spleen fell following CpG treatment ($0.1 \pm 0.06 \times 10^6$ cells per spleen in PBS-treated vs $0.04 \pm 0.2 \times 10^6$ in CpG-treated; $P = .02$). However, the $H6pdh^{-/-}$ to $H6pdh^{+/+}$ ratio for pDC origin switched from 2.5 ± 0.8 in steady state to 1.2 ± 0.2 in CpG-treated chimeras ($P < .001$; Figure 4). Although splenic pDCs are quiescent in the steady state, parabiotic studies indicate they also have a shorter half-life (<3 days) than other DC populations.[28] Furthermore, we observed increased splenic pDC turnover following CpG treatment in nonchimeric mice, as evaluated following continuous exposure to 5-bromo-2′-deoxyuridine and measurement of its incorporation in gated B220$^+$PDCA-1$^+$SiglecH$^+$ cells (at 24 hours, % 5-bromo-2′-deoxyuridine positive, $1.5\% \pm 0.6\%$ in PBS-treated vs $8.0\% \pm 5.0\%$

in CpG 1826–treated mice; n = 6; $P = .04$). Taken together, these data explain the rapid shift in ratios with treatment by CpG and indicate that cell-intrinsic regulation of pDC survival by H6PDH in the steady state is overridden upon TLR9 activation.

H6PDH regulates myeloid DC immunostimulatory potential in vivo

To test whether prereceptor amplification of GCs regulates other properties of DCs, we performed further studies focusing on the ability of DCs to activate naive T cells. In initial experiments, we generated immature or LPS-matured BM-derived DCs from $H6pdh^{-/-}$ mice and $H6pdh^{+/+}$ littermate controls. As shown in Figure 5A, exposure to B at 10^{-7} M impaired the maturation of BM DCs to LPS from both groups, whereas exposure to A at 10^{-7} M blocked the differentiation of wild-type but not $H6pdh^{-/-}$ cells. Immature and LPS-matured BM DCs from $H6pdh^{-/-}$ mice and $H6pdh^{+/+}$ mice that had been cultured in the absence of A or B were pulsed with Kb-restricted OVA peptide (SIINFEKL) and injected intraperitoneally into B6 mice before determination of the endogenous anti-OVA T-cell response at day 7 by pentamer and ELISPOT. In

Figure 4. H6PDH regulates splenic pDC survival in the steady but not inflammatory state. (A) The frequency of pDCs (as a percentage of live gated cells) in spleen and lymph nodes (LN) of $H6pdh^{+/+}$ versus $H6pdh^{-/-}$ mice. (B) The frequency of pDCs (as a percentage of live gated cells) in spleen and lymph nodes of ($H6pdh^{+/+} \rightarrow H6pdh^{+/+}$) versus ($H6pdh^{-/-} \rightarrow H6pdh^{+/+}$) BM chimeras 12 weeks after reconstitution. (C) $H6pdh^{+/+}$ (CD45.1):$H6pdh^{-/-}$ (CD45.2)$\rightarrow H6pdh^{+/+}$ (CD45.1) mixed BM chimeras were evaluated 12 to 16 weeks after hematopoietic reconstitution and 24 hours after treatment with intraperitoneal PBS or CpG 1826. (Left) Representative contour plots showing plasmacytoid dendritic cell antigen-1 (PDCA-1) and sialic acid binding immunoglobulin-like lectin H (SiglecH) staining in a pregated B220$^+$ splenocyte population. (Middle) Representative flow cytometric histograms showing CD45.1 staining in gated B220$^+$PDCA-1$^+$SiglecH$^+$ cells. (Right) Summary of pooled data showing percentage of pDCs derived from $H6pdh^{-/-}$ (CD45.2) or $H6pdh^{+/+}$ (CD45.1) BM. Data derived from 3 independent experiments.
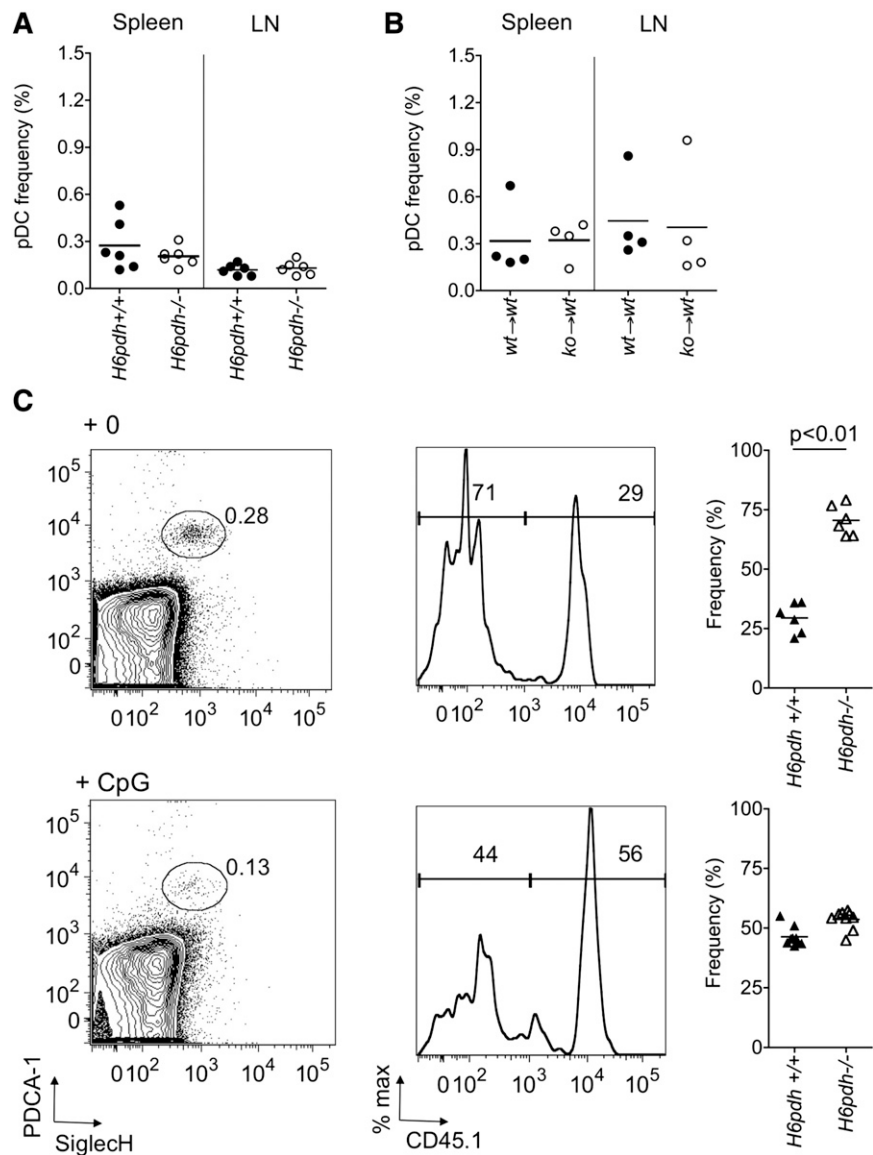
comparison with control cells, both immature and mature BM DCs from $H6pdh^{-/-}$ mice increased the frequencies of CD8 T cells able to bind pentamer and generate IFN-γ to specific peptides (Figure 5B-C).

H6PDH regulates CD8α$^+$ DC functions in vivo

To test whether this inhibitory function of the 11βHSD1-H6PDH pathway was also applicable to naturally occurring myeloid DCs, we next isolated CD11c^{high} DCs from untreated $H6pdh^{-/-}$ and $H6pdh^{+/+}$ mice and used them to stimulate naive T cells ex vivo following their preexposure to physiologic concentrations of A or B (Figure 6A; supplemental Figure 1, available on the *Blood* Web site). Whereas preexposure to both A and B blocked the immunostimulatory capacity of $H6pdh^{+/+}$ CD11c^{high} DCs, $H6pdh^{-/-}$ CD11c^{high} DCs were resistant to the effects of A as we had observed for BM DCs. Because we had previously observed much higher levels of 11βHSD1 reductase in CD8α$^+$ rather than CD8α$^-$ DC sub-populations, we examined the phenotypes of these subsets in ($H6pdh^{+/+}$:$H6pdh^{-/-} \rightarrow H6pdh^{+/+}$) mixed chimeras. In the steady state, the CD8α$^+$ subpopulation derived from knockout BM de-

monstrated a slight trend for increased surface expression of CD86 staining compared with wild-type cells. In contrast, lack of H6PDH made no difference to the phenotype of CD8α$^-$ DCs. To determine whether prereceptor amplification of GCs would influence maturation of DCs in response to inflammatory cues, we also treated mixed chimeras by intraperitoneal injection with CpG 1826. As shown in Figure 6B, CD8α$^+$ DCs, but not CD8α$^-$ DCs, derived from $H6pdh^{-/-}$ BM demonstrated enhanced CD86 upregulation at 24 hours after injection compared with wild-type DCs.

We reasoned that prereceptor amplification of GCs by CD8α$^+$ DCs represents a cell-autonomous checkpoint with the potential to regulate T-cell stimulatory capacity. To test this concept, we evaluated OVA-specific CD8 T-cell responses following CD8α$^+$ DC-targeted vaccination in the presence or absence of carbenoxalone (CBX), an 11βHSD1 inhibitor. In this experimental system, CD8α$^+$ DCs are targeted through injection of anti-DEC205:OVA antibody.[23] Cross-presentation of OVA antigen by CD8α$^+$ DCs in the steady state induces only abortive T-cell proliferation, whereas presentation in the presence of DC-activating stimuli leads to productive immunity.[23] As shown in Figure 7A-B, anti-DEC205:OVA elicited only a very minor
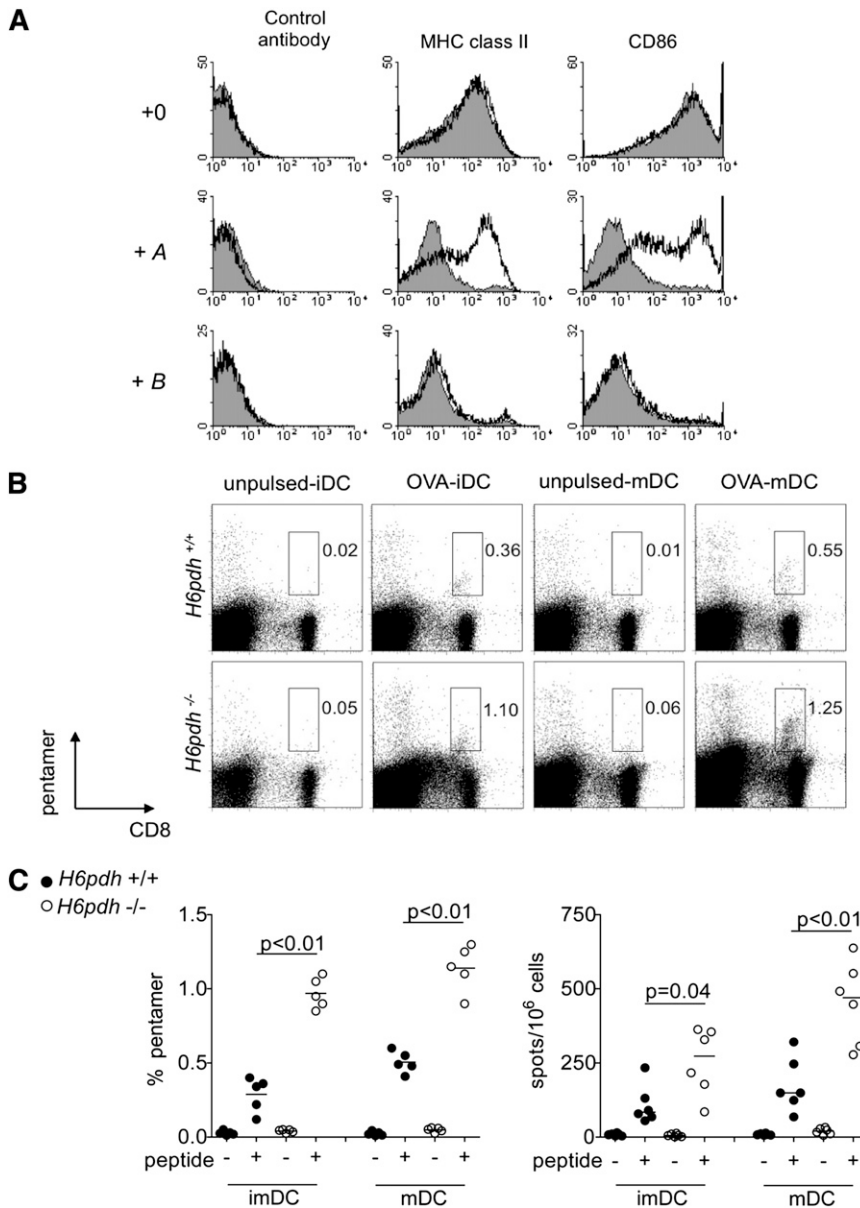
Figure 5. H6PDH regulates the differentiation and immunostimulatory potential of BM-derived DCs. (A) $H6pdh^{-/-}$ (open histograms) or $H6pdh^{+/+}$ littermate (solid gray histograms) BM-derived DCs were exposed to 2 μg/mL LPS in the presence or absence of 10^{-7} M *A* or 10^{-7} M *B*. Representative staining for MHC class II and CD86 in gated CD11c$^+$ BM DCs from mice. (B-C) Immature DCs (iDCs) or LPS-matured BM DCs (mDCs) from $H6pdh^{-/-}$ or $H6pdh^{+/+}$ littermate control mice were untreated or pulsed with 1 μM SIINFEKL peptide before intraperitoneal injection into B6 mice. At 7 days, the host anti-OVA response was evaluated by Kb:SIINFEKL pentamer staining and by ELISPOT assay for specific IFN-γ generation. (B) Representative dot plots of pentamer staining. (C) Summary graphs for Kb:SIINFEKL pentamer and ELISPOT evaluations. Data are pooled from 3 independent experiments.

endogenous OVA-specific CD8 T-cell response when given alone. When anti-DEC205:OVA was administered together with CBX, we observed a significant but modest increase in the endogenous response compared with anti-DEC205:OVA alone. In a parallel experiment, we also evaluated cytotoxicity of the host anti-OVA response by determining in vivo killing of B cells differentially labeled with carboxyfluorescein succinimidyl ester (CFSE) and pulsed with relevant or irrelevant peptide (n = 2/ group). No specific cytotoxicity was observed in mice receiving CpG or CBX alone or in immunized mice receiving anti-DEC205: OVA or anti-DEC205:OVA plus CBX. To determine how 11βHSD1 inhibition would influence the CD8 T-cell response in the presence of adjuvant, we cotreated mice with CpG 1826, which also binds to DEC205 and gains rapid access to the TLR9-containing endosomal compartment.[29] When anti-DEC205:OVA was combined with intraperitoneal CpG, the antigen-specific response, as measured by pentamer frequency and IFN-γ generation, was modestly increased compared with antibody. However, when CBX treatment was combined with anti-DEC205:OVA and CpG, a synergistic increase in the response was observed in both pentamer numbers and in their capacity to produce IFN-γ. Specific in vivo cytotoxicity was observed in both groups of immunized mice receiving the CpG stimulus (mean, 69% specific cytotoxicity in the anti-DEC205:OVA plus CpG group and 86% in the anti-DEC205:OVA plus CpG plus CBX group; n = 2 per group). Because T cells also possess high levels of 11βHSD1 reductase activity,[25] we also performed control experiments in which we evaluated the responses of transferred $H6pdh^{-/-}$ and $H6pdh^{+/+}$ OT-I cells following anti-DEC205:OVA immunization with or without the addition of intraperitoneal CpG. Baseline responses to immunization did not differ between wild-type and knockout OT-I cells, nor was there any difference between the groups in the presence of CpG, indicating that the prereceptor amplification of GC by T cells did not regulate their activation in this system (supplemental Figure 2). Taken together, these data indicate that pharmacologic inhibition of 11βHSD1 in the context of DC vaccination enhances priming of naive antigen-specific CD8 T cells.

Figure 6. H6PDH regulates the differentiation and immunostimulatory potential of spleen CD11c$^+$ DCs. (A) CD11c$^+$ DCs were sorted from spleens of H6pdh$^{-/-}$ or H6pdh$^{+/+}$ littermate control mice and incubated in normal media alone (+0) or in the presence of 10^{-7} M A or 10^{-7} M B for 18 hours before pulsing with OVA$_{323-339}$ peptide (or irrelevant peptide) for 2 hours. DCs were then washed and cells were used at the indicated ratios in stimulation assays with 1×10^5 carboxyfluorescein succinimidyl ester (CFSE) –labeled OT-II CD4 cells for 96 hours. (Top) Flow cytometric histograms from a representative experiment showing CFSE staining of gated T cells incubated with H6pdh$^{+/+}$ or H6pdh$^{-/-}$ CD11c$^+$ DCs in the presence of vehicle (left), 10^{-7} M A (middle) or 10^{-7} M B (right) at a DC: T-cell ratio of 1:4 (n = 3 independent experiments). Values in the upper left corner show mean ± SD for the average number of T-cell divisions calculated for each group. Bar in upper right corner indicates the position of undivided cell sets according to CFSE staining of T cells incubated with DC pulsed with irrelevant peptide. (Bottom) Histograms showing summary data for the average number of T-cell divisions at different DC:T-cell ratios as a percentage of maximum (at a DC:T-cell ratio of 1:2) under each experimental condition. Quantitative data showing absolute numbers of divided T cells per well according to genotype of stimulator DC and exposure to A or B are shown in supplemental Figure 1. (B) Representative histograms for CD86 staining in gated MHC class II^{high} CD11c^{high} splenic CD8α$^+$ DCs or CD8α$^-$ DCs from H6pdh$^{-/-}$ (CD45.2):H6pdh$^{+/+}$ (CD45.1)→H6pdh$^{+/+}$ (CD45.1) mixed BM chimeras that were evaluated 12 to 16 weeks after hematopoietic reconstitution and 24 hours after intraperitoneal treatment with nil or CpG. Staining for each DC subset derived from H6pdh$^{-/-}$ (bold black line, open histograms) or H6pdh$^{+/+}$ (thin black line, solid gray histograms) BM is shown. Summary data from 3 independent experiments are shown to the right of each set of histograms.
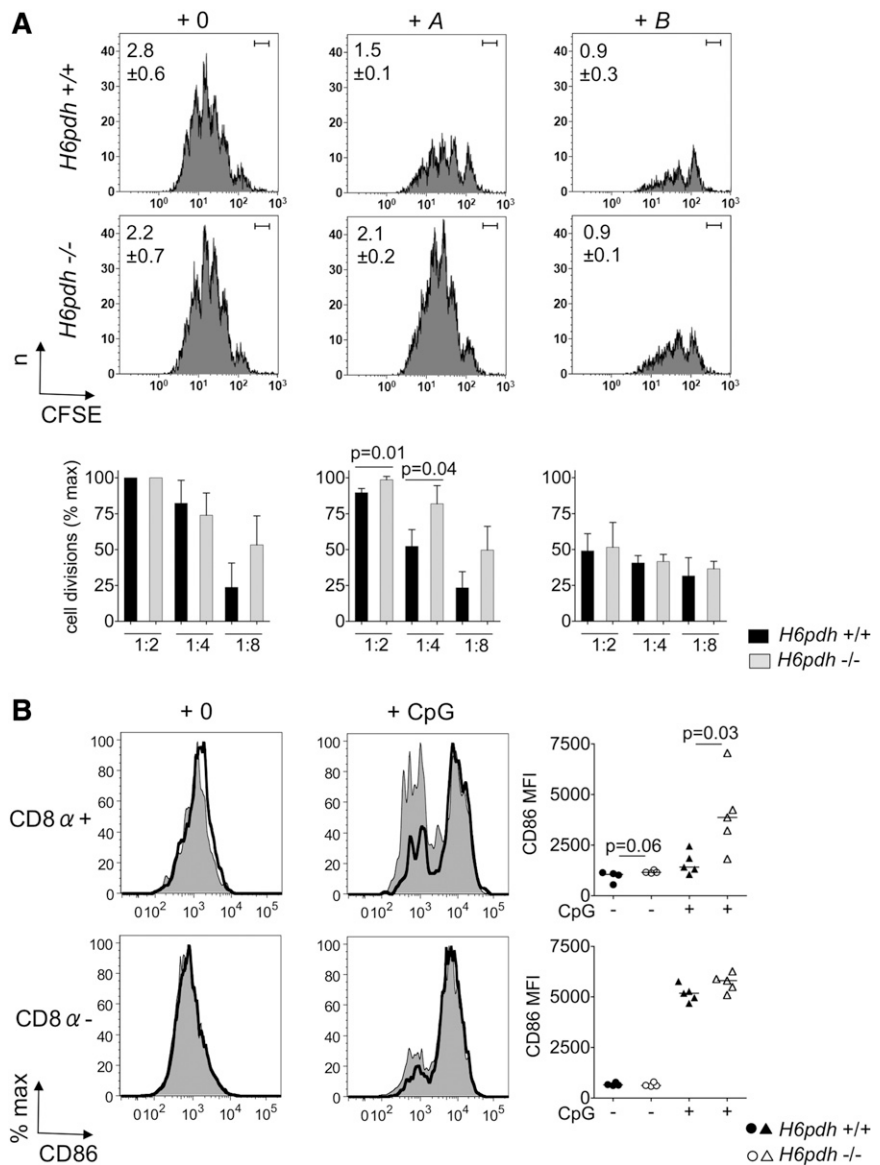
Discussion

In this study, we have shown that murine pDCs and CD8α$^+$ DCs are highly proficient in amplifying levels of active corticosterone in both steady and inflammatory states. Under physiologic conditions, this property restricts the survival of the pDC population through a cell-intrinsic mechanism, an effect that is overridden following TLR-mediated activation. Prereceptor amplification of GCs by CD8α$^+$ DCs reduces their capacity to mature in response to microbial stimuli and to stimulate naive T cells. Pharmacologic inhibition of this molecular pathway enhances adaptive T-cell responses following vaccination, a finding with therapeutic relevance.

Our data indicate an important distinction between DCs and other cells in their capacity to mediate prereceptor GC amplification. Thus, stromal and epithelial cells possess low constitutive ability to generate corticosterone, but this increases sharply following nuclear factor κB activation by proinflammatory stimuli.[30] TLR-mediated activation of tissue macrophages also increases their 11βHSD1 reductase activity,[31] in this case, promoting phagocytosis of apoptotic

cells such as neutrophils.[32] Taken together, these findings suggest that upregulation of 11βHSD1-H6PDH activity within tissues is important in promoting resolution of inflammation and avoidance of immunopathology. Consistent with this concept, mice lacking 11βHSD1 are prone to excessive tissue injury induced by sterile inflammation.[33] In contrast, prereceptor GC amplification by DC is constitutive and already maximal in steady state, with little influence from exposure to additional innate or adaptive immune stimuli. Our data instead indicate a role for the 11βHSD1-H6PDH complex in DC homeostasis and/or regulating functions at the initiation of an immune response rather than during its resolution.

We have demonstrated that H6PDH can regulate pDC survival through both intrinsic and extrinsic mechanisms. The relative contribution of each mechanism is likely to depend upon microenvironmental constraints such as cell proximity and the potential of other cell types to convert A→B. Although BM chimera experiments showed that H6PDH expression in hematopoietic cells did not regulate the overall size of the pDC compartment in secondary lymphoid organs, it did have a cell-intrinsic role in restricting the efficiency with which pDCs occupied the steady state niche (Figure 4C). This function was
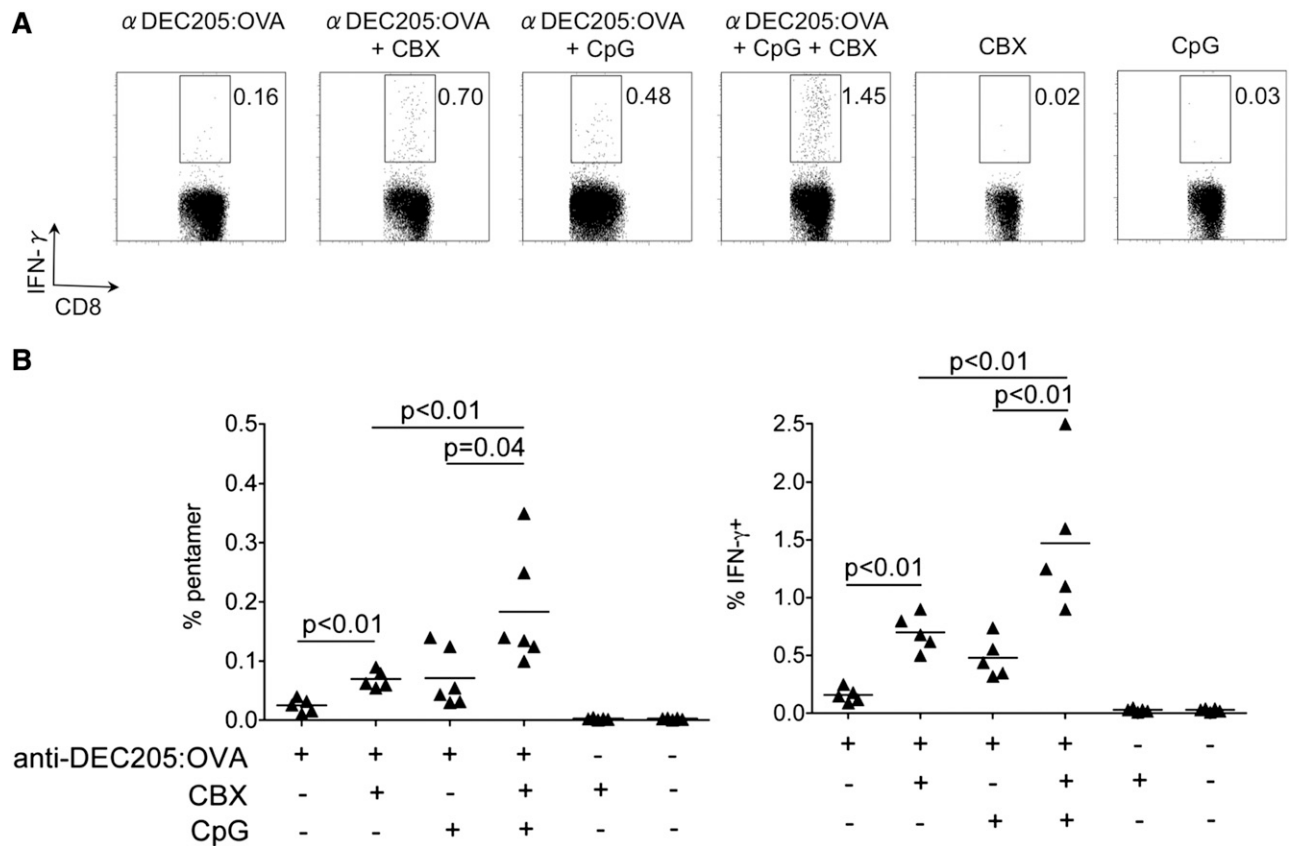
Figure 7. Transient inhibition of 11βHSD1 enhances capacity of CD8α⁺ to cross-present antigen. Wild-type female B6 mice were treated with one or more of anti-DEC205:OVA (200 μL supernatant), CBX (2 mg), or CpG 1826 (100 μg) given by intraperitoneal injection before evaluating the endogenous anti-OVA CD8 T-cell response 7 days later. (A) Representative flow cytometric plots showing intracellular IFN-γ staining on gated CD8 T cells following restimulation overnight with relevant (SIINFEKL) or irrelevant peptide. Gates set according to irrelevant peptide. (B) Summary data for by Kb:SIINFEKL pentamer staining (left) in spleens or specific intracellular IFN-γ generation (right) are shown.

redundant upon CpG-mediated activation, a finding consistent with other recent studies demonstrating tumor necrosis factor α– and IFN-α–dependent increases in pro-survival molecules following TLR activation.[8,26] Importantly, activated pDCs secreted equivalent amounts of IFN-α upon CpG activation, irrespective of whether H6PDH was intact or disabled. Because activation of pDCs is associated with autoimmunity in both experimental[34] and clinical contexts,[26,35-37] H6PDH-mediated regulation of survival within steady-state niches might be an important checkpoint to prevent excessive type I IFN responses to innocuous stimuli or during the initial phases of a viral infection.

Prereceptor GC amplification regulated the phenotype and function of CD8α⁺ DCs more than the CD8α⁻ subset, a finding that correlated with higher 11βHSD1 reductase activity. It is noteworthy, that CD8α⁺ DCs and their immediate precursors also appear most sensitive to the effects of chronically elevated corticosterone in stressed mice,[38] influencing both survival and the ability of mature cells to cross-present antigen. In our experiments, temporary inhibition of 11βHSD1 activity in a model of CD8α⁺ DC-mediated cross-presentation following targeted vaccination also demonstrated a role for this pathway in enhancing the priming of naive T-cell activation. The synergy between CBX-mediated inhibition of 11βHSD1 and TLR activation via CpG implies that they promote distinct pathways involved in antigen cross-presentation of antigen and/or T-cell stimulation. In this regard, CBX treatment alone has little effect on expression of proinflammatory cytokines, chemokines, or MHC molecules in BM DCs, suggesting that other molecular pathways are

involved.[39] It is unlikely that the mechanism involves the potential for CBX to inhibit gap junctions,[40] because these effects would be predicted to have a negative rather than positive effect on cross-presentation.[41] However, confirmation that the positive effects of CBX on DC vaccination are specific to the inhibition of 11βHSD1 in CD8α⁺ DCs rather than another cell type will require inducible systems permitting control of 11βHSD1 or H6PDH expression in specific tissues.

In conclusion, we reason that the 11βHSD1-H6PDH pathway in DCs is required to prevent spontaneous or excessive inflammation in the steady state or excessive immunopathology following infection. Transient, pharmacologic inhibition of this pathway may have therapeutic potential in provoking immunity following vaccination. Therefore, it will be important to explore the immune adjuvant activity of the novel, selective 11βHSD1 inhibitors that are being tested for their efficacy in metabolic syndrome and diabetes.[42]

Authorship

Correspondence: Ronjon Chakraverty, Transplantation Immunology Group, Department of Haematology, Cancer Institute and Institute of Immunity and Transplantation, University College London, London, United Kingdom; e-mail: r.chakraverty@ucl.ac.uk.

References

1. Webster JI, Tonelli L, Sternberg EM. Neuroendocrine regulation of immunity. *Annu Rev Immunol.* 2002;20:125-163.

2. Szatmari I, Nagy L. Nuclear receptor signalling in dendritic cells connects lipids, the genome and immune function. *EMBO J.* 2008;27(18):2353-2362.

3. Matyszak MK, Citterio S, Rescigno M, Ricciardi-Castagnoli P. Differential effects of corticosteroids during different stages of dendritic cell maturation. *Eur J Immunol.* 2000;30(4):1233-1242.

4. Piemonti L, Monti P, Allavena P, et al. Glucocorticoids affect human dendritic cell differentiation and maturation. *J Immunol.* 1999; 162(11):6473-6481.

5. Rea D, van Kooten C, van Meijgaarden KE, Ottenhoff TH, Melief CJ, Offringa R. Glucocorticoids transform CD40-triggering of dendritic cells into an alternative activation pathway resulting in antigen-presenting cells that secrete IL-10. *Blood.* 2000;95(10):3162-3167.

6. Woltman AM, de Fijter JW, Kamerling SW, Paul LC, Daha MR, van Kooten C. The effect of calcineurin inhibitors and corticosteroids on the differentiation of human dendritic cells. *Eur J Immunol.* 2000;30(7):1807-1812.

7. Truckenmiller ME, Princiotta MF, Norbury CC, Bonneau RH. Corticosterone impairs MHC class I antigen presentation by dendritic cells via reduction of peptide generation. *J Neuroimmunol.* 2005;160(1-2):48-60.

8. Lepelletier Y, Zollinger R, Ghirelli C, et al. Toll-like receptor control of glucocorticoid-induced apoptosis in human plasmacytoid predendritic cells (pDCs). *Blood.* 2010;116(18):3389-3397.

9. Seckl JR, Morton NM, Chapman KE, Walker BR. Glucocorticoids and 11beta-hydroxysteroid dehydrogenase in adipose tissue. *Recent Prog Horm Res.* 2004;59:359-393.

10. Oakley RH, Cidlowski JA. Cellular processing of the glucocorticoid receptor gene and protein: new mechanisms for generating tissue-specific actions of glucocorticoids. *J Biol Chem.* 2011;286(5): 3177-3184.

11. Tomlinson JW, Walker EA, Bujalska IJ, et al. 11beta-hydroxysteroid dehydrogenase type 1: a tissue-specific regulator of glucocorticoid response. *Endocr Rev.* 2004;25(5):831-866.

12. Cao Y, Bender IK, Konstantinidis AK, et al. Glucocorticoid receptor translational isoforms underlie maturational stage-specific glucocorticoid sensitivities of dendritic cells in mice and humans. *Blood.* 2013;121(9):1553-1562.

13. Cima I, Corazza N, Dick B, et al. Intestinal epithelial cells synthesize glucocorticoids and regulate T cell activation. *J Exp Med.* 2004; 200(12):1635-1646.

14. Vacchio MS, Ashwell JD. Thymus-derived glucocorticoids regulate antigen-specific positive selection. *J Exp Med.* 1997;185(11):2033-2038.

15. Gathercole LL, Lavery GG, Morgan SA, Cooper MS, Sinclair AJ, Tomlinson JW, Stewart PM. 11β-hydroxysteroid dehydrogenase 1: translational and therapeutic aspects. *Endocr Rev.* 2013;34(4): 525-555.

16. Atanasov AG, Nashev LG, Schweizer RA, Frick C, Odermatt A. Hexose-6-phosphate dehydrogenase determines the reaction direction of 11beta-hydroxysteroid dehydrogenase type 1 as an oxoreductase. *FEBS Lett.* 2004;571(1-3):129-133.

17. Bánhegyi G, Benedetti A, Fulceri R, Senesi S. Cooperativity between 11beta-hydroxysteroid dehydrogenase type 1 and hexose-6-phosphate dehydrogenase in the lumen of the endoplasmic reticulum. *J Biol Chem.* 2004;279(26):27017-27021.

18. Draper N, Walker EA, Bujalska IJ, et al. Mutations in the genes encoding 11beta-hydroxysteroid dehydrogenase type 1 and hexose-6-phosphate dehydrogenase interact to cause cortisone reductase deficiency. *Nat Genet.* 2003;34(4):434-439.

19. Freeman L, Hewison M, Hughes SV, Evans KN, Hardie D, Means TK, Chakraverty R. Expression of 11beta-hydroxysteroid dehydrogenase type 1 permits regulation of glucocorticoid bioavailability by human dendritic cells. *Blood.* 2005;106(6):2042-2049.

20. Lavery GG, Walker EA, Draper N, et al. Hexose-6-phosphate dehydrogenase knock-out mice lack 11 beta-hydroxysteroid dehydrogenase type 1-mediated glucocorticoid generation. *J Biol Chem.* 2006;281(10):6546-6551.

21. Gilliet M, Boonstra A, Paturel C, et al. The development of murine plasmacytoid dendritic cell precursors is differentially regulated by FLT3-ligand and granulocyte/macrophage colony-stimulating factor. *J Exp Med.* 2002;195(7):953-958.

22. Goold HD, Escors D, Conlan TJ, Chakraverty R, Bennett CL. Conventional dendritic cells are required for the activation of helper-dependent CD8 T cell responses to a model antigen after cutaneous vaccination with lentiviral vectors. *J Immunol.* 2011;186(8):4565-4572.

23. Bonifaz LC, Bonnyay DP, Charalambous A, et al. In vivo targeting of antigens to maturing dendritic cells via the DEC-205 receptor improves T cell vaccination. *J Exp Med.* 2004;199(6):815-824.

24. Miller JC, Brown BD, Shay T, et al; Immunological Genome Consortium. Deciphering the transcriptional network of the dendritic cell lineage. *Nat Immunol.* 2012;13(9):888-899.

25. Zhang TY, Ding X, Daynes RA. The expression of 11 beta-hydroxysteroid dehydrogenase type I by lymphocytes provides a novel means for intracrine regulation of glucocorticoid activities. *J Immunol.* 2005;174(2):879-889.

26. Guiducci C, Gong M, Xu Z, et al. TLR recognition of self nucleic acids hampers glucocorticoid activity in lupus. *Nature.* 2010;465(7300):937-941.

27. Lavery GG, Hauton D, Hewitt KN, Brice SM, Sherlock M, Walker EA, Stewart PM. Hypoglycemia with enhanced hepatic glycogen synthesis in recombinant mice lacking hexose-6-phosphate dehydrogenase. *Endocrinology.* 2007;148(12):6100-6106.

28. Liu K, Waskow C, Liu X, Yao K, Hoh J, Nussenzweig M. Origin of dendritic cells in peripheral lymphoid organs of mice. *Nat Immunol.* 2007;8(6):578-583.

29. Lahoud MH, Ahmet F, Zhang JG, et al. DEC-205 is a cell surface receptor for CpG oligonucleotides. *Proc Natl Acad Sci USA.* 2012; 109(40):16270-16275.

30. Ahasan MM, Hardy R, Jones C, et al. Inflammatory regulation of glucocorticoid metabolism in mesenchymal stromal cells. *Arthritis Rheum.* 2012;64(7):2404-2413.

31. Thieringer R, Le Grand CB, Carbin L, Cai TQ, Wong B, Wright SD, Hermanowski-Vosatka A. 11 Beta-hydroxysteroid dehydrogenase type 1 is induced in human monocytes upon differentiation to macrophages. *J Immunol.* 2001;167(1):30-35.

32. Gilmour JS, Coutinho AE, Cailhier JF, et al. Local amplification of glucocorticoids by 11 beta-hydroxysteroid dehydrogenase type 1 promotes macrophage phagocytosis of apoptotic leukocytes. *J Immunol.* 2006;176(12):7605-7611.

33. Coutinho AE, Gray M, Brownstein DG, et al. 11β-Hydroxysteroid dehydrogenase type 1, but not type 2, deficiency worsens acute inflammation and experimental arthritis in mice. *Endocrinology.* 2012;153(1):234-240.

34. Gregorio J, Meller S, Conrad C, et al. Plasmacytoid dendritic cells sense skin injury and promote wound healing through type I interferons. *J Exp Med.* 2010;207(13):2921-2930.

35. Rönnblom L, Pascual V. The innate immune system in SLE: type I interferons and dendritic cells. *Lupus.* 2008;17(5):394-399.

36. Tucci M, Quatraro C, Lombardi L, Pellegrino C, Dammacco F, Silvestris F. Glomerular accumulation of plasmacytoid dendritic cells in active lupus nephritis: role of interleukin-18. *Arthritis Rheum.* 2008;58(1):251-262.

37. Wenzel J, Tüting T. An IFN-associated cytotoxic cellular immune response against viral, self-, or tumor antigens is a common pathogenetic feature in "interface dermatitis". *J Invest Dermatol.* 2008; 128(10):2392-2402.

38. Hunzeker JT, Elftman MD, Mellinger JC, Princiotta MF, Bonneau RH, Truckenmiller ME, Norbury CC. A marked reduction in priming of cytotoxic CD8+ T cells mediated by stress-induced glucocorticoids involves multiple deficiencies in cross-presentation by dendritic cells. *J Immunol.* 2011;186(1):183-194.

39. Endong L, Shijie J, Sonobe Y, et al. The gap-junction inhibitor carbenoxolone suppresses the differentiation of Th17 cells through inhibition of IL-23 expression in antigen presenting cells. *J Neuroimmunol.* 2011;240-241:58-64.

40. de Groot JR, Veenstra T, Verkerk AO, et al. Conduction slowing by the gap junctional uncoupler carbenoxolone. *Cardiovasc Res.* 2003;60(2):288-297.

41. Heath WR, Carbone FR. Coupling and cross-presentation. *Nature.* 2005;434(7029):27-28.

42. Sun D, Wang M, Wang Z. Small molecule 11β-hydroxysteroid dehydrogenase type 1 inhibitors. *Curr Top Med Chem.* 2011;11(12):1464-1475.